Tripping Effects in Low-Reynolds Number Turbulent Boundary Layers

R. Örlü[1], C. Sanmiguel Vila[2], R. Vinuesa[1],S. Discetti[2], A. Ianiro[2] and P. Schlatter[1]
[1]*Linné FLOW Centre, KTH Mechanics, SE-100 44 Stockholm, Sweden.*
[2]*Aerospace Engineering Group, Universidad Carlos III de Madrid, Leganés, Spain.*

ramis@mech.kth.se

Abstract

This paper presents a study focused on the development of zero-pressure-gradient turbulent boundary layers (ZPG TBL) towards canonical conditions in the low Reynolds-number range. Six different tripping configurations are employed including weak, late and strong overtripping covering a Reynolds-number range (based on momentum thickness) of $500 < Re_\theta < 4,000$. Evolution of the mean streamwise and variance profiles of the different TBLs is studied. Convergence towards a canonical state of the different tripping devices is determined using a new method based on the diagnostic-plot concept (Alfredsson *et al.*, 2011), which only requires mean and turbulence intensity measurements within the outer layer. Existing methods in the literature which rely on empirical skin-friction and shape-factor curves are used to validate the proposed diagnostic-plot method. Contrary to these methods, the present one does not require knowledge of the skin-friction coefficient, shape factor or wake parameter, which would need accurate measurements of friction velocity, wall position and full profile measurements in order to compute integral quantities.

1 Introduction

The assessment of effects such as inflow conditions, tripping devices and development length on the characteristics of zero pressure gradient (ZPG) turbulent boundary layers (TBLs) has started to receive some attention in recent years (see *e.g.* Hutchins, 2012; Schlatter and Örlü, 2012; Marusic *et al.*, 2015).

The problem is extremely relevant since, as stated by Chauhan *et al.* (2009), such effects may lead to local non-equilibrium conditions, producing flows which are no longer representative of the canonical ZPG TBL. Chauhan *et al.* (2009) analysed a vast number of experimental databases, and assessed the streamwise evolution of the wake parameter Π (Coles, 1962) and the shape factor $H = \delta^*/\theta$ (where δ^* and θ are the displacement and momentum thicknesses, respectively), obtained from fits to a composite profile formulation. Comparison of the Π and H trends with the numerical integration of the composite profile allowed them to obtain a criterion to identify well-behaved profiles, *i.e.*, not affected by such non-equilibrium effects.

Interestingly, Schlatter and Örlü (2010) showed that numerical databases are also affected by inflow conditions and tripping method, which explained the observed differences up to 5% in H and up to 20% in the skin friction coefficient C_f, when comparing a wide number of direct numerical numerical simulation (DNS) databases of ZPG TBLs. In a follow-up study, Schlatter and Örlü (2012) also reported that if transition is initiated at Reynolds numbers Re based on momentum thickness $Re_\theta < 300$, then comparisons between different numerical and experimental databases can be made for $Re_\theta > 2,000$ if the flow is not severely over or undertripped (see also Örlü and Schlatter, 2013). Thus, under these conditions the ZPG TBL can be considered as *canonical*, and does not exhibit features reminiscent of its particular inflow condition.

A comparison of the evolution from three ZPG TBLs, tripped with three different tripping devices, was carried out by Marusic *et al.* (2015). In this study a standard sand paper trip was considered, together with two threaded rods designed to overstimulate the boundary layer, and it was found that the effects of the trip remained up to streamwise distances on the order of $2,000$ trip heights (conclusion valid for their particular setup and trip method). Such effects were manifested on the large-scale motions in the flow.

Rodriguez-Lopez *et al.* (2016) studied the effect of different tripping configurations with the aim of generating canonical high-Re TBLs. A sawtooth serrated fence and different spanwise arrays of cylinders were employed to obtain a uniform wall-normal blockage distribution case and a non-uniform one. It was shown that tripping configurations with a uniform blockage ratio can be used to obtain canonical high-Re TBLs with an increase of up to 150% in momentum thickness with respect to a standard sandpaper trip.

A numerical equivalent of the aforementioned studies can be found in the work by Sillero *et al.* (2013), who reported that in one of their preliminary simulations the computational box was not long enough to allow full development of the ZPG TBL, the most prominent effect being observed in the larger scales of the flow. In their case, the inflow condition was generated through a rescaling method, different from the volume force tripping employed by Schlatter and Örlü (2010, 2012) in their simulations.

The present investigation revisits the early experimental studies on the history effects of tripping devices on turbulence characteristics at low Re (see *e.g.* Erm & Joubert, 1991) in light of the recent numerical as well as high Re experimental studies with the aim to a) assess the various criteria proposed in the literature to discern a canonical ZPG TBL and b) propose a practical method that can be employed prior to extensive measurements and/or DNS as required by present methods. For this purpose new wind tunnel experiments with six different tripping configurations have been performed, which are described in Sec. 2, and discussed and summarised in Sec. 3 and 4, respectively.

Tripping characteristics & location	Symbol code	Identification
DYMO 'V' @ 75 mm	Red	weak tripping
DYMO 'V' @ 230 mm	Green	late tripping
DYMO 'V' @ 75, 90, 110 mm & 5 mm square bar @ 85 mm	Blue	strong overtripping
DYMO 'V' @ 90, 110 mm & 2.4 mm height turbulator	Black	optimal 1
DYMO 'V' @ 90, 110 mm & 1.6 mm height turbulator	Magenta	optimal 2
DYMO 'V' @ 90 mm	Cyan	weak/late tripping

Table 1: Specifications of the tripping configurations including location and respective colour coding for symbols. The embossed (DYMO) letter 'V' points into the flow direction and has a nominal height of 0.3 mm

2 Experimental setup

The experimental data was obtained in the Minimum Turbulence Level (MTL) closed-loop wind tunnel located at the Royal Institute of Technology (KTH) in Stockholm, which has a 7 m long test section with a cross-sectional area of 0.8×1.2 m^2 with a streamwise velocity disturbance level less than 0.025% of the free-stream velocity. The boundary layer developed on a flat plate suspended 25 cm above the tunnel floor under a zero pressure gradient condition that was established through adjustment of the ceiling.

A variation of DYMO tape (with the embossed letter 'V' and a width of 9 mm with a maximum thickness of 0.5 mm) arrangements in various combinations with and w/o turbulators has been used to establish 5 different evolutions of TBLs (listed in Table 1) similar to those studied numerically in Schlatter and Örlü (2012), *i.e.*, a combination of weak, late, and strong trippings. Additionally, a square bar of length 5 mm was used to mimic a strongly overtripped case. All the tripping configurations were placed spanning the full spanwise length of the plate and at a streamwise location in the range $75 < x/\text{mm} < 230$ from the leading edge, corresponding to the range $130 < Re_\theta < 260$.

Single-point streamwise velocity measurements were performed by means of a single in-house hot-wire probe with a Platinum wire of 560 μm length and nominal diameter of 2.5 μm. These dimensions provided sufficient spatial resolution (the wire length being smaller than 20 viscous units for all considered cases) to ensure meaningful comparisons of the higher-order turbulence statistics.

A set of 4 streamwise locations was selected for each tripping configuration with few additional stations to match Re_θ, covering a range of $500 < Re_\theta < 4,000$. Care was taken to acquire sufficient measurement points within the viscous sublayer and the buffer region in order to correct for the absolute wall position and determine the friction velocity (Örlü *et al.*, 2010; Alfredsson, *et al.*, 2011b) without the need to rely on log-law constants for the mean velocity profile (*i.e.* Clauser chart method). A sampling frequency and time of 20 kHz and 30 s, respectively, were employed in all the velocity measurements, and a low-pass filter of 10 kHz cut-off frequency was used prior to the data acquisition in order to avoid aliasing.

To compute boundary-layer quantities in a consistent manner, the procedure outlined in Schlatter and Örlü (2010) was followed: The composite profile by Nickels (2004) was used to obtain the freestream velocity U_∞ and the 99% boundary-layer thickness δ_{99}. Reynolds numbers and integral quantities were then computed using the fitted composite profile. In the present study the superscript '+' denotes scaling with the friction velocity u_τ or the viscous length $\ell^* = \nu/u_\tau$ (where $u_\tau = \sqrt{\tau_w/\rho}$, τ_w being the mean wall-shear stress, ρ is the fluid density and ν is the kinematic viscosity).

3 Results and discussion

A compilation of the streamwise mean and variance profiles for the various trippings is shown in Figure 1a-b) and depicts a clear collapse of the mean velocity profile within the inner layer. This is in accordance with Schlatter and Örlü (2012), which showed that the near-wall region (*e.g.* in terms of the skin friction or the root mean square (rms) of the fluctuating wall shear stress) quickly adapts to that of a canonical TBL. The outer layer instead, exhibiting strong variations in the mean and variance profiles, requires as expected a much longer development length to forget about its specific tripping history. In particular, the strong overtripping case shows an outer peak which is a particular feature due to the square bar used as a disturbance.

The differences in the boundary-layer evolution can be better appreciated when considering the ratios of the various boundary-layer thicknesses as shown in Figure 1c), where clearly the late and strong overtripping cases exhibit the largest discrepancies from all other cases thereby indicating that even their most downstream station has not adapted to the canonical state.

In order to determine when a TBL profile has reached a canonical state various criteria have been proposed in the literature. Among those are *e.g.* the evolution of the shape factor H, the skin-friction coefficient C_f, and the wake parameter Π, common references quantities (Chauhan *et al.*, 2009). These quantities are assumed to provide a measure of when the boundary layers recover from the different boundary and inflow conditions employed. The problem with these quantities is the need to estimate with enough accuracy variables such as the wall position y_w and the friction velocity u_τ. These parameters are typically difficult to measure directly and accurately and highly sensitive to experimental errors. Furthermore, in the low Reynolds-number range the evolution of the reference quantities H or Π can be defined in terms of several empirical curves, thus inheriting further uncertainties.

For these reasons, here an alternative scaling is employed, the so-called diagnostic plot (Alfredsson *et al.*, 2011a, 2012), where the root mean square of the streamwise velocity fluctuation scaled by its mean $\sqrt{\langle uu \rangle}/U$ is plotted against the mean velocity U normalised by the free-stream velocity U_∞ rather than the wall distance, as shown in Figure 2a). This scaling has shown promising results to scale (among others) canonical ZPG TBL data covering a wide Re_θ range throughout the logarithmic and wake layers (Örlü *et al.*, 2016). One of the key points of this scaling is the fact that, according to Alfredsson *et al.* (2011a), the data of canonical ZPG TBL collapse in the outer region for $U/U_\infty \leq 0.9$, following a linear relation,

$$\frac{\sqrt{\langle uu \rangle}}{U} = \alpha - \beta \frac{U}{U_\infty}, \qquad (1)$$

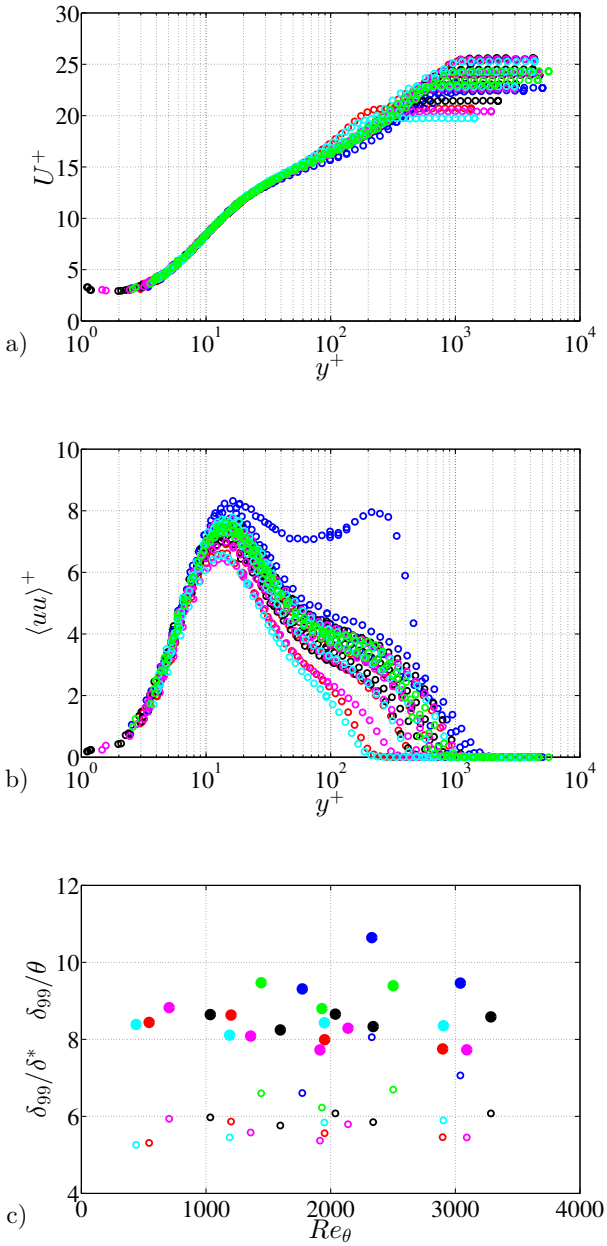

Figure 1: Inner-scaled a) mean and b) variance profile as well as the corresponding c) ratio of boundary layer thickness (δ_{99}) to displacement thickness (δ^*, open symbols) and momentum-loss thickness (θ, filled symbols) for the entire data set (see Table 1 for colour code).

where α and β are positive fitting constants, which have an asymptotic value of $\alpha \simeq 0.278$ and $\beta \simeq 0.242$ for $Re_\theta > 2,000$ in the present study.

In light of the success to scale canonical wall-bounded turbulence data (Örlü *et al.*, 2016), the profiles which follow equation (1) can be considered as canonical cases. Using this new criterion the only information required to use this method are U and $\sqrt{\langle uu \rangle}$ in the outer region, and U_∞. As a consequence, there is no need to obtain parameters such as y_w or u_τ, nor to measure entire velocity profiles.

In Figure 2a) all velocity profiles are presented in the diagnostic plot, while in Figure 2b) only those that adhere to the established linear trend given through equation (1) are reported. By omitting the profiles that do not adhere to the linear scaling in the outer region, clear Re_θ-trends in both the mean and variance profiles are revealed (Figure 3a–b), and the differences among Re-evolutions of the boundary layer thicknesses diminish as apparent from Figure 3c). The diagnostic-plot scaling is also applied in Figure 4 to the DNS of Schlatter and Örlü (2012), which consider the same Re_θ range and similar trip configurations with the idea of extending the diagnostic-plot method to DNS data.

In order to validate the results from the diagnostic-plot scaling, the shape factor H and the skin-friction coefficient C_f evolution with Re_θ proposed by Monkewitz *et al.* (2007) and Chauhan *et al.* (2009), respectively, are evaluated in Figure 5. It can be observed that the profiles that follow the diagnostic-plot criterion, *i.e.*, the ones shown in Figure 3 and 4, both comply with the reference C_f curve and also the H curve within $\pm 3\%$ and 2%, respectively, as shown in Figure 5. This is an argument for the fact that the diagnostic-plot criterion provides a robust criterion to discern whether a particular boundary layer exhibits canonical ZPG TBL conditions. All profiles which do not follow the diagnostic-plot criterion either fail according to the C_f or the H based criteria.

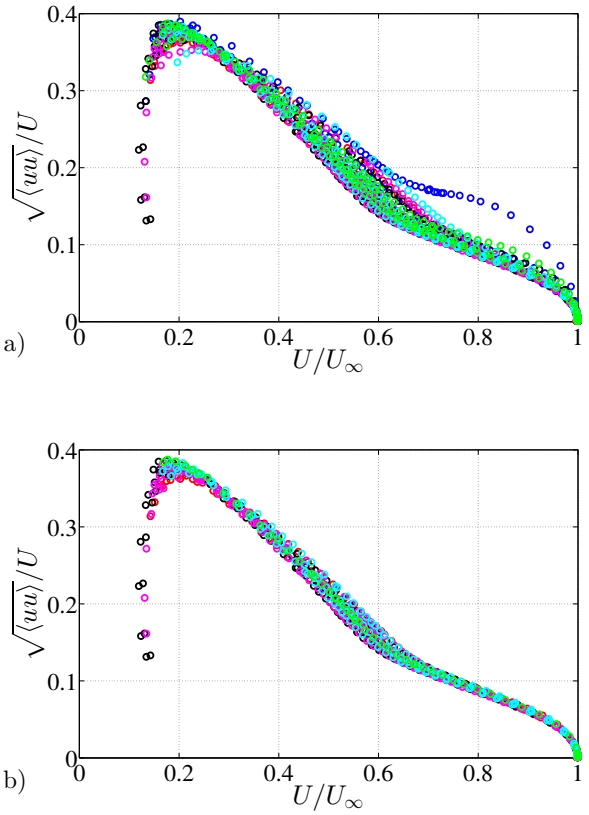

Figure 2: Extended diagnostic plot for a) the entire data set and b) the data that complies with the diagnostic-plot scaling. Note that the region $U/U_\infty < 0.2$ corresponds to the viscous sublayer, as apparent from the misreadings of the hot-wire anemometer in the vicinity of the wall (Alfredsson and Örlü, 2010)

For example, from Figure 5 it can be observed that the cases which fulfil the H criterion (such as the lowest Re profile from the strong overtripping case) but not not the C_f criterion are clearly discarded by the diagnostic-plot approach.

The previous discussion shows that the diagnostic-plot method is consistent with the reference methods employed in the literature with the advantage that it only requires measurements of the streamwise mean velocity and its turbulence intensity relatively far from the wall, where measurements are most accurate and straightforward. This method appears suitable to be employed prior to extensive measurements and/or DNS to discern when a TBL can be considered canonical or not. Since the outer layer in the diagnostic scaling (besides being linear) is Re-invariant when $Re_\theta > 2,000$, a streamwise scan through the outer layer of the TBL (which practically can easily be determined) would immediately reveal from which streamwise location on the boundary layer would adhere to that of a canonical ZPG TBL, without the necessity to measure full profiles.

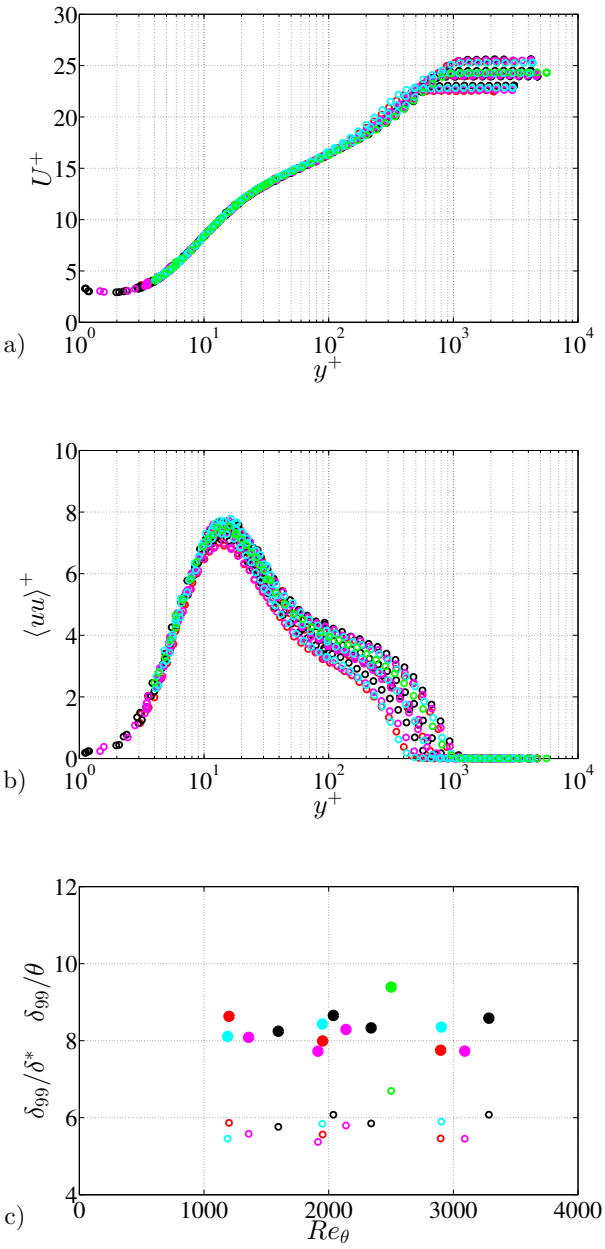

Figure 3: Same quantities as in figure 1 for experimental profiles that fulfil the diagnostic scaling in the outer layer (see Figure 2)

4 Conclusions

The transition to a canonical state of zero-pressure-gradient TBLs is assessed in the present paper through the study of the evolution of six differently tripped ZPG TBLs. Streamwise velocity profiles are measured over the Reynolds number range $500 < Re_\theta < 4,000$, and their evolutions from the various inflow conditions are compared at several streamwise locations downstream of the flat-plate leading edge. The determination of the canonical development of the different profiles is assessed by means of the diagnostic-plot method proposed by Alfredsson *et al.* (2011a). The diagnostic-plot methodology proposed in the present study for the study of tripping effects is therefore a reliable and straightforward technique to evaluate the development of ZPG TBLs towards canonical conditions, which only requires measurements of the mean streamwise velocity and its turbulence intensity in the outer region of the boundary layer. This is a great advantage in comparison to methods based on the skin-friction coefficient, shape factor or wake parameter, which require more involved measurements of friction velocity, accurate wall position and full profile measurements in order to compute integral quantities.

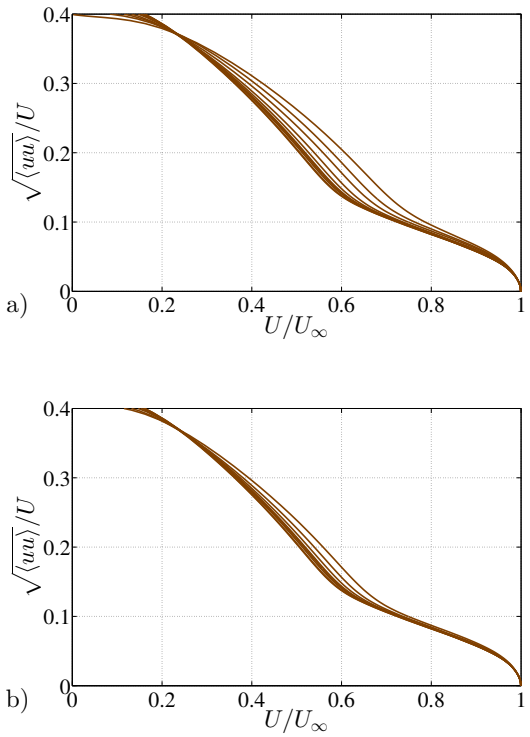

Figure 4: Extended diagnostic plot for the DNS data (Schlatter and Örlü, 2012): a) all the DNS data and b) the data that complies with the diagnostic-plot scaling

Acknowledgments

RÖ, RV and PS acknowledge the financial support from the Swedish Research Council (VR), the Knut and Alice Wallenberg Foundation, and the Lundeqvist foundation. CSV acknowledges the financial support from Universidad Carlos III de Madrid within the program "Ayudas para la Movilidad del Programa Propio de Investigación". CSV, SD and AI were partially supported by the COTURB project (Coherent Structures in Wall-bounded Turbulence), funded by the European Research Council Coturb Grant No. ERC-2014.AdG-669505.

References

Alfredsson, P. H. and Örlü, R. (2010) The diagnostic plot–a litmus test for wall bounded turbulence data. *Eur. J. Fluid Mech. B/Fluids*, Vol. 42, pp. 403–406.

Alfredsson, P. H., Segalini, A. and Örlü, R. (2011a) A new scaling for the streamwise turbulence intensity in wall-bounded turbulent flows and what it tells us about the "outer" peak. *Phys. Fluids*, Vol. 23, pp. 041702.

Alfredsson, P. H., Örlü, R. and Segalini, A. (2012) A new formulation for the streamwise turbulence intensity distribution in wall-bounded turbulent flows. *Eur. J. Fluid Mech. B/Fluids*, Vol. 36, pp. 167–175.

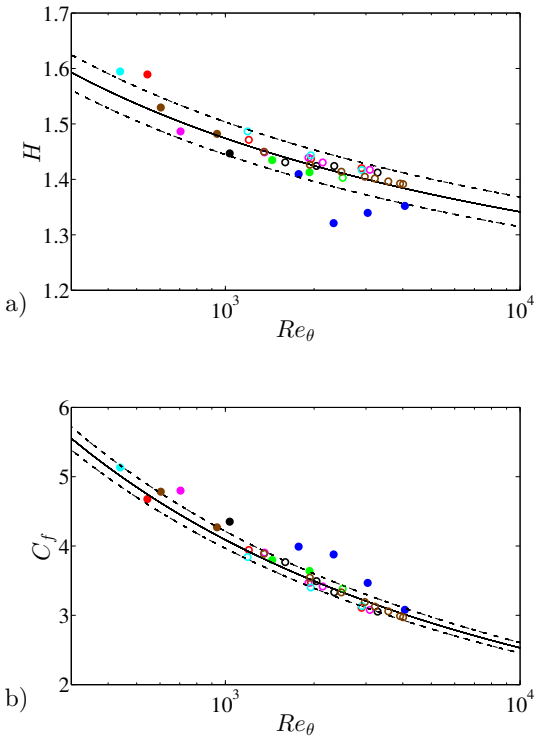

Figure 5: a) Shape factor H and b) skin-friction coefficient $C_f \times 10^3$ evolution with Re_θ for the entire trip data set and the DNS from Schlatter and Örlü (2012). Filled symbols are the profiles that do not follow the diagnostic-plot scaling given by equation (1). Solid lines are the references for H and C_f proposed by Monkewitz *et al.* (2007) and Chauhan *et al.* (2009) and the dashed lines show ±2% and ±3% tolerances, respectively

Alfredsson, P. H., Örlü, R. and Schlatter, P. (2011b) The viscous sublayer revisited–exploiting self-similarity to determine the wall position and friction velocity. *Exp. Fluids*, Vol. 51, pp. 271–280.

Chauhan, K. A., Monkewitz, P. A. and Nagib, H. M. (2009), Criteria for assessing experiments in zero pressure gradient boundary layers, *Fluid Dyn. Res.*, Vol. 41, pp. 021404.

D. E. Coles, The turbulent boundary layer in a compressible fluid (1962), *Rand. Rep. R-403-PR.*

Erm, L. P. and Joubert, P. N. (1991) Low-Reynolds-number turbulent boundary layers, *J. Fluid Mech.*, Vol. 230, pp 1–44.

Hutchins, N. (2012) Caution: Tripping hazards, *J. Fluid Mech.*, Vol. 710, pp. 1–4.

Marusic, I., Chauhan, K. A., Kulandaivelu, V. and Hutchins, N. (2015), Evolution of zero-pressure-gradient boundary layers from different tripping conditions, *J. Fluid Mech.*, Vol. 783, pp. 379–411.

Monkewitz, P. A., Chauhan, K. A. and Nagib, H. M. (2007), Self-consistent high-Reynolds-number asymptotics for zero-pressure-gradient turbulent boundary layers, *Phys. Fluids*, Vol. 19, pp. 115101.

Nickels, T. B. (2004), Inner scaling for wall-bounded flows subject to large pressure gradients, *J. Fluid Mech.*, Vol. 521, pp. 217–239.

Örlü, R., Fransson, J. H. M. and Alfredsson, P. H. (2010), On near wall measurements of wall bounded flows–the necessity of an accurate determination of the wall position, *Prog. Aerosp. Sci.*, Vol. 46, pp. 353–387.

Örlü, R. and Schlatter, P. (2013) Comparison of experiments and simulations for zero-pressure gradient turbulent boundary layers at moderate Reynolds numbers. *Exp. Fluids*, Vol. 54, pp. 1547.

Örlü, R., Segalini, A., Klewicki, J. and Alfredsson, P. H. (2016) High-order generalisation of the diagnostic plot to turbulent boundary layers. *J. Turbul.* Vol. 17, pp. 664–677.

Rodríguez-López, E., Bruce, P. J. K. and Buxton, O. R. H. (2016), On the formation mechanisms of artificially generated high Reynolds number turbulent boundary layers, *Boundary-Layer Meteor.*, Vol. 160, pp. 201–224.

Schlatter, P. and Örlü, R. (2010), Assessment of direct numerical simulation data of turbulent boundary layers, *J. Fluid Mech.*, Vol. 659, pp. 116–126.

Schlatter, P. and Örlü, R. (2012), Turbulent boundary layers at moderate Reynolds numbers: inflow length and tripping effects, *J. Fluid Mech.*, Vol. 710, pp. 5–34.

Sillero, J. A., Jiménez, J. and Moser, R. D. (2013), One-point statistics for turbulent wall-bounded flows at Reynolds numbers up to $\delta^+ \simeq 2000$, *Phys. Fluids*, Vol. 25, pp. 105102.